Tribology International 150 (2020) 106360

Contents lists available at ScienceDirect

Tribology International

journal homepage: http://www.elsevier.com/locate/triboint

Effect of cation nature on vacuum tribo-degradation and lubrication performances of two tetrafluoroborate ionic liquids

Yi Li [a,b], Songwei Zhang [a,c,*], Qi Ding [a,c], Litian Hu [a,**]

[a] State Key Laboratory of Solid Lubrication, Lanzhou Institute of Chemical Physics, Chinese Academy of Sciences, Lanzhou, 730000, PR China
[b] Center of Materials Science and Optoelectronics Engineering, University of Chinese Academy of Sciences, Beijing 100049, PR China
[c] Qingdao Center of Resource Chemistry & New Materials, Qingdao, 266071, PR China

ARTICLE INFO

Keywords:
Ionic liquids
Vacuum tribo-decomposition behaviors
Tribochemical reaction mechanisms
Vacuum lubrication

ABSTRACT

Vacuum lubrication and tribo-degradation performance investigations of two imidazolium tetrafluoroborate ionic liquids (ILs, LAB103 and LB104), were systematically conducted by the VFBT-4000 vacuum four-ball tribometer equipped with a quadrupole mass spectrometer. They both have quite wide liquid range with high thermostability and good fluidity at low temperature. Results of vacuum tribological tests show that LAB103 present better lubricity and lower corrosivity as compared with that of LB104, due to its strong adsorption layers and robust tribofilms on worn surfaces. Tribo-degradation test results exhibit that the decomposition of ILs is mainly caused by frictional stimulus. The decomposition products partially diffuse to vacuum chamber, being captured by mass spectrometer detector and others participate in the tribochemical reactions.

1. Introduction

Many mechanical assemblies used in space vehicles, such as satellites, spaceships, interplanetary probes and space station, rely on high-performance lubricants to provide reliable lubrication throughout their mission lives [1,2]. For example, nut-screw, momentum wheel and gyroscope, which operated at high speed or worked in boundary lubrication regime. Obviously, liquid lubricants would be a better choice for these mechanisms. Longer life, higher reliability and better performance of liquid lubricants are increasingly required, due to the high cost and unrepairable during the operating for these space vehicles. Space lubrication for mechanisms in low earth orbit (LEO) always involves many special working conditions, including high vacuum, high/low temperatures, variety radiations, upper atmosphere, etc. The high vacuum environment, which is about 10^{-5}–10^{-7} Pa in LEO and ~10^{-4} Pa inside the space capsule, may induce the liquid lubricants to evaporate rapidly. Then, environment temperature of space varies commonly in the range of −150–150 °C, which will be the demanding condition for liquid lubricants.

Ionic liquids (ILs) show negligible volatility, excellent thermal stability and non-flammability, and have great potential application as lubricants or lubricant additives in space lubrication area. Since 2001, Liu's group presented that ILs were excellent liquid lubricants for variety of materials [3], such as, Si_3N_4/sialon ceramics, steel/copper, steel/-steel, steel/sialon ceramics, steel/SiO_2, hundreds of papers were published on this topic [4–8]. In our research experience, the lubricating performances in vacuum showed huge difference from those in air under boundary lubrication [9–12]. Space lubricants commonly failed in the way of excessive tribo-decomposition of lubricants.

The degradation of IL lubricants under frictional stimulus might produce dual effects on their performances. Firstly, tribochemical reactions would occur between the substrates and IL molecules or decomposition pieces from IL molecules. These products form tribochemical films, which further resulting in good lubrication performances [12–16]. Secondly, these pieces were volatile products, which easily diffused in vacuum, polluting other components and speed up the degradation process of IL lubricants [17–19]. Before using ILs as space lubricants, it is necessary to make it clear that (1) How did the frictional stimulus cause the decomposition of IL molecules? (2) How did the functional group and test conditions affect the degradation paths?

In this work, the vacuum lubrication performances and tribo-degradation behaviors of two imidazolium tetrafluoroborate ILs with

* Corresponding author. State Key Laboratory of Solid Lubrication, Lanzhou Institute of Chemical Physics, Chinese Academy of Sciences, Lanzhou, 730000, PR China.
** Corresponding author.
E-mail addresses: zhangsw@licp.cas.cn (S. Zhang), lthu@licp.cas.cn (L. Hu).

https://doi.org/10.1016/j.triboint.2020.106360
Received 20 February 2020; Received in revised form 29 March 2020; Accepted 3 April 2020
Available online 12 April 2020
0301-679X/

alkyl and alkenyl were comparatively investigated. By means of several modern analysis methods, the mechanisms of lubrication and degradation of two ILs were also investigated.

2. Experimental specifics

2.1. Preparation and characterization of materials

The chemical structures of two imidazolium tetrafluoroborate ILs are shown in Fig. 1. [BMIM][BF_4] (LB104) was obtained from Lanzhou Institute of Chemical Physics, Chinese Academy of Sciences. [AMIM][BF_4] (LAB103) was synthesized referred to the reference [20]. NMR spectrometer with superconducting magnet (^{1}HNMR, ^{13}CNMR), high resolution mass spectra (HRMS) were developed to characterize the molecular structure of two ILs, and results are as follows:

Then, we tested the kinematic viscosities of ILs on a low temperature viscometer and an automatic viscometer. The phrase transition temperatures of ILs was carried out on differential thermal scanner (DSC) from −150 °C to +80 °C in N_2 at the heat-up rate of 10 °C/min. The pour points were evaluated by an automatic pour point tester using GB/T 3535 procedures. The thermal gravimetric analyzer (TG) was employed to study the thermal stability from 25 °C to 600 °C in N_2 at the heat-up rate of 10 °C/min.

2.2. Vacuum friction and tribo-degradation tests

The vacuum lubrication performances and tribo-degradation processes of two ILs were investigated on the VFBT-4000 vacuum four-ball tribometer equipped with quadrupole mass spectrometer (QMS). Four identical steel balls were selected as frictional pairs, the size of which was Φ12.7 mm (1/2 in). In addition, the surface roughness of each AISI 52100 steel ball was 0.025 μm with a hardness of HRC 59–62. Approximately 10 ml ILs was used to ensure the contact areas of four steel balls were fully covered by the IL lubricants for each test. All the tests were conducted at the temperature of 15–25 °C with the velocity of 1450 ± 10 rpm under the applied load of 100 N or 400 N. All the test balls and holders should be totally cleaned in petroleum ether (b.p.: 60–90 °C) ultrasonically.

The duration of each vacuum tribological test under ~10^{-5} Pa was 30 min. After the friction test, optical microscope was used to measure the diameters of wear scar on the three lower steel balls. In this work, the wear scar diameter (WSD) value was calculated by averaging the wear scar diameters. To ensure the repeatability, at least three uniform tribological tests should be reduplicated.

Tribo-degradation processes were characterized by surveying volatile products emission during the friction process through QMS method. A series of mechanical pump and turbo molecular pump were employed to obtain the high vacuum system (~10^{-5} Pa). To reach the balanced background atmosphere, it should be kept for at least 3 h with the QMS on before the test began. Afterwards, the volatile products in different periods (before, during and after the friction process) were collected, and each period was assigned for 8 min. Before friction process, for each

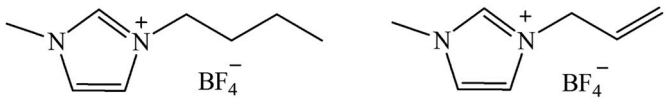

LB104 ([BMIm][BF_4]) LAB103 ([AMIm][BF_4])

Fig. 1. Chemical structures of synthesized ionic liquids.
^{1}H NMR (400 MHz, $(CD_3)_2CO$): δ 8.93 (s, 1H), 7.70 (s, 1H), 7.68 (s, 1H), 6.13 (m, 1H), 5.46 (m, 1H), 5.40 (m, 1H), 4.97 (d, 2H), 4.03 (s, 3H).
^{13}C NMR (101 MHz, $(CD_3)_2CO$): δ136.78, 131.31, 124.01, 122.42, 120.62, 51.40, 35.71.
m/z: 123.0914([AMIm]$^+$), 297.0996([AMIm][BF_4^-]$_2$).

mass-to-charge ratio m/z of constituent part in mass spectra, we would collected at least 6 spectra for each test to determine the statistically valid data of the background, $I_b(m/z)$, and standard deviation, $\sigma_b(m/z)$. During and after the friction process, we calculated the differential mass spectrometry (DMS) spectra of mass components by subtracting $\bar{I}_b(m/z)$ from the collected DMS spectra:

$$\Delta I(m/z,\ t) = I(m/z,\ t) - \bar{I}_b(m/z)$$

Herein, changes of the each component as a function of time caused by frictional stimulus were represented as the DMS spectra. What's more, in order to abandon random variations, the DMS spectra were filtered as follows:

$$\Delta I(m/z,\ t) = \Delta I(m/z,\ t),\ \text{if } [SN(m/z,\ t)] > 5;$$

$$\Delta I(m/z,\ t) = 0,\ \text{if } [SN(m/z,\ t)] \le 5$$

Herein, $SN(m/z,\ t) = I(m/z,\ t)/\sigma_b(m/z)$, which represents the signal-to-noise ratio of the corresponding mass component in the DMS spectra at a specific moment t.

2.3. Characterization and analysis

The scanning electron microscopy (SEM) and three-dimensional optical surface profiler (3D) were employed to measure the topographies of wear scar surfaces on the steel balls. The chemical states of elements on the wear scar surfaces were detected by X-ray photoelectron spectrometer (XPS). The calibration binding energies of elements in this paper was 284.8 eV for C1s.

3. Results and discussion

3.1. Physicochemical properties

The physicochemical properties of two ILs were summarized and listed in Table 1. The data reveals that both ILs present high viscosity index value (>120), indicating good viscosity-temperature performances. The DSC and TG spectra of ILs are also presented in Fig. 2. DSC measurement results shows that two ILs have low glass transition temperatures with the value of −88 °C (LB104) and −94 °C (LAB103) and low pour points (T_p) both lower than −66 °C. It could be found from TG analysis results that thermal decomposition temperatures of both ILs were higher than 340 °C. Results demonstrated that both LB104 and LAB103 have wide liquid range with high thermal stability and good low-temperature fluidity.

3.2. Vacuum friction and wear properties of ILs

The vacuum lubrication performances of two ILs under low and high loads are summarized and presented in Fig. 3. For the conventional IL LB104, the friction coefficient curves fluctuated obviously during the whole friction process under either high or low load, indicating that relatively intense tribochemical reactions are induced by frictional stimulus. For the functionalized IL LAB103 at 100 N, the friction

Table 1
Physicochemical properties of ILs.

Items		ILs	
		LB104	LAB103
Kinematic viscosity/cSt	−30 °C	9016.41	2223.94
	40 °C	30.28	16.26
	100 °C	5.57	3.88
Viscosity index		124	136
Glass transition temperature/°C		−88	−94
Pour point/°C		<-66	<-66
Thermal decomposition temperature/°C		377	353

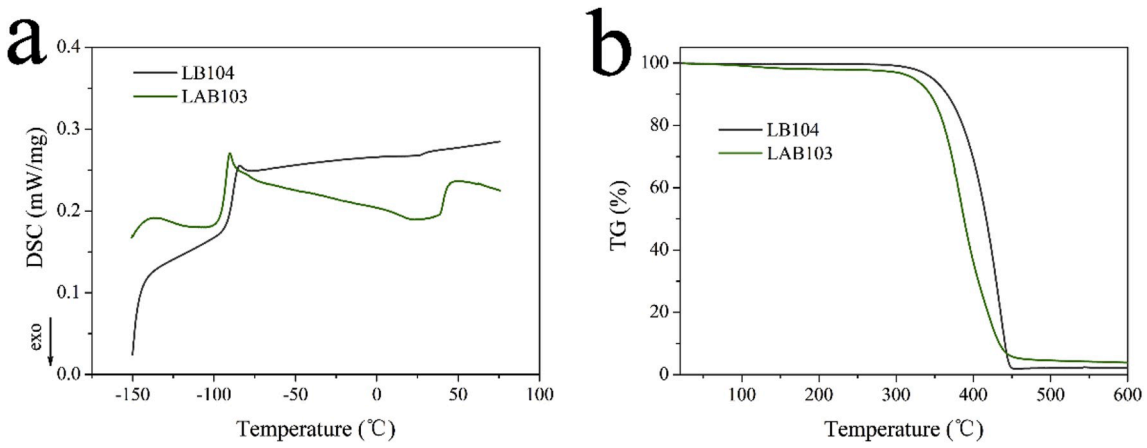

Fig. 2. DSC and TG spectra of two ILs: (a) DSC; (b) TG.

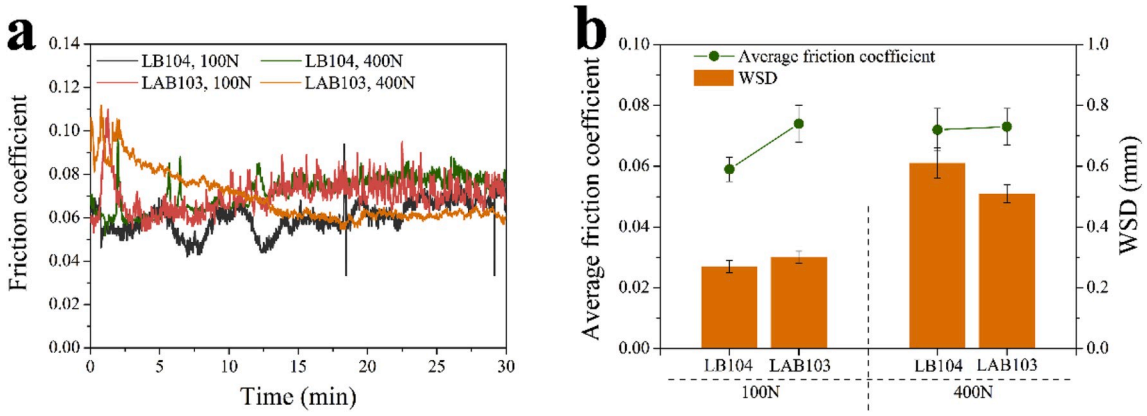

Fig. 3. The vacuum lubrication performances of two ILs under low and high loads: (a) friction coefficient curves as functions of time; (b) average friction coefficient and WSD.

coefficient curve reached a relatively stable value after a short running-in period. It is interesting that a low and stable friction coefficient curve was obtained by LAB103 under higher load after a long running-in period. Results illustrate that tribochemical reactions between IL LAB103 and substance surface lead to good lubricating performances, especially under severe conditions, but these chemical reactions are not as intense as LB104. In Fig. 3b, LB104 performs lower values about average friction coefficient and WSD than those of LAB103 at 100 N. While the load increases to 400 N, smaller wear scar is obtained by LAB103 compared with LB104. These results from Fig. 3 show that LAB103 exhibits better anti-wear capacity and friction-reducing performance than LB104 under severer conditions.

For a deeper insight of the lubrication performances, the topographies of worn surfaces detected by SEM and 3D are presented in Fig. 4. In Figs. 4a and 4b, tremendous corrosion pits are seen on the wear scar surface for LB104 at 100 N, indicating intense corrosive tribochemical reactions. It can also be proved by the rough wear tracks in Fig. 4c. While being lubricated by LB104 at 400 N, large wear scars with severe wear loss and many deep wear traces are found in Figs. 4d–4f. In Figs. 4g–4i, smooth surface with clear wear trace are detected on the wear scar surface for LAB103 at 100 N. An unusual phenomenon is found in Figs. 4j–4l that an irregular oval-shaped wear scar with minor wear loss on the worn surface lubricated by LAB103 under the load of 400 N. It can be deduced that while LAB103 is used under higher load, these strong and continuous tribofilms can bear up severe conditions, providing good lubrication properties for frictional pairs.

To examine lubrication mechanism and ascertain the chemical composition of the boundary tribofilms, XPS analysis of representative elements was performed. In Figs. 5a and 5b, Fe 2p and F 1s peaks existing at 711.3 eV and 685.0 eV can be attributed to Fe and F in FeF_2 [21]. Results confirmed that tribochemical reactions between F-containing fragments of ILs and steel surfaces occurred to form tribochemical products FeF_2 inside the contact area during the sliding process for both ILs. In Fig. 5c, N 1s peaks would be identified as N-containing organic compounds (alkylammonium at 410.0 eV and organic amine at 399.8eV) [21], indicating that N-containing organic compounds were generated on the wear scar surfaces of the frictional balls through the tribo-decomposition and tribo-polymerization processes for both ILs during the friction process. In Fig. 5d, no obvious B 1s peaks are detected under these specific test conditions, which illustrates that no B-containing tribochemical products are found on the worn steel surfaces for both ILs. And the XPS survey spectra of the worn surfaces were presented in Fig. 6.

Combining these results of vacuum tribological tests and the characterization of worn surfaces, XPS results are further discussed. For LB104 under different loads, more FeF_2 were found on the wear scar surface under the load of 100 N than that at 400 N, while less N-containing compounds formed on the worn surfaces under both loads than those for LAB103. It indicated that under the load of 100 N, intense tribochemical interactions between F-containing fragments of ILs LB104 and worn surfaces, which induced severe corrosion to steel ball. However, tribo-products were mostly swept from the worn surfaces by the high contact stress, producing high friction and severe wear of frictional ball under the higher load of 400 N. For the worn surfaces lubricated by LAB103 under both loads, less FeF_2 were found than that for LB104 at 100 N, and more N-containing compounds were detected than that for

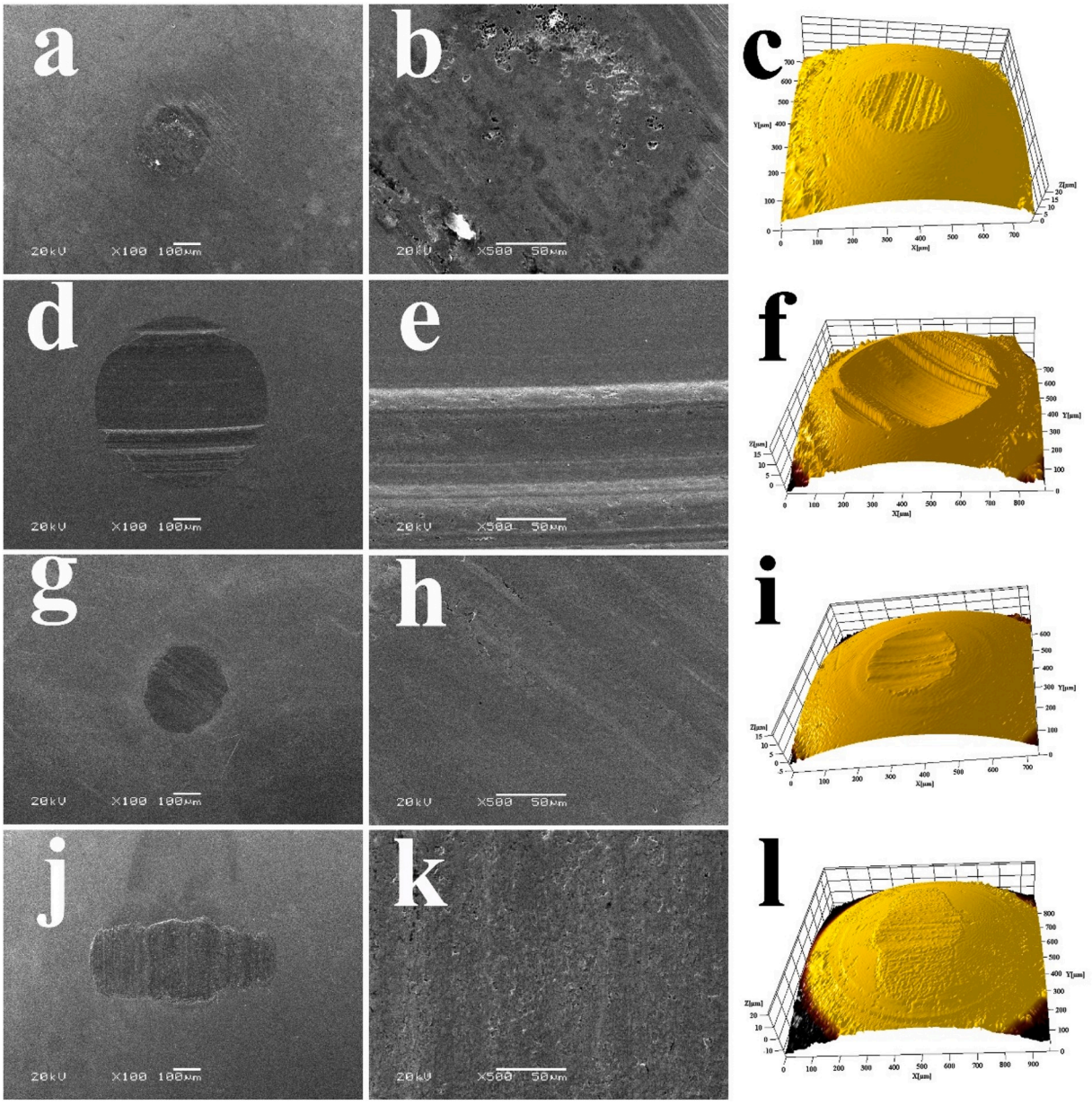

Fig. 4. The topographies of worn surfaces detected by SEM and 3D lubricated at different conditions: (a–c) LB104, 100 N; (d–f) LB104, 400 N; (g–i) LAB103, 100 N; (j–l) LAB103, 400 N.

LB104 under both loads. This indicated that ILs and IL fragments of LAB103 formed strong adsorption layers on the contact zone, which could effectively inhibit the corrosive attack of F-containing fragments to the steel surfaces, yielding good lubrication performances under both low and high loads.

3.3. Vacuum tribo-decomposition behaviors of ILs

Figs. 7 and 8 showed the DMS spectra for LB104 and LAB103 obtained during different periods of friction process, and the error bars in Figs. 7a, 7d, 8a and 8d denoted standard deviation (σ). It is a difficult task to identify all volatile spectral components as the decomposition products of IL molecules accurately, due to the overlapping of ion fragments of different volatile products. Yet there are still some components that can be surely identified. The *m/z* 2 peak belonged to H_2^+, which was consistent with these earlier results reported by Mori et al. [22] and Nevshupa et al. [23]. These peaks of *m/z* 12–16 were primarily vested in CH_x^+ (x = 0–4), while these spectral peaks at 26–30 and 38–44 were determined as a mixture of C_2 and C_3 alkanes, alkenes or fragments. Additionally, peaks of *m/z* 28 and 44 advise the existence of CO^+ and CO_2^+, correspondingly. The occurrence of higher alkanes and/or alkenes, which might be owing to the recombination of lower alkenes, would be deduced from these peaks of *m/z* 54–56. These peaks of *m/z* 31, 45 and 46 were vested in CH_3O^+, $C_2H_5O^+$, $C_2H_5OH^+$, correspondingly. The ion fragments CF^+ would be concluded from the spectral peak of *m/z* 31. Peaks of *m/z* 81 and 82 were determined as N-methylimidazole ion fragments ($[(C_3H_3N_2)CH_2]^+$and $[(C_3H_3N_2)CH_3]^+$). The group peaks at *m/z* 66–68 in Fig. 8d belonged to imidazole ring ion fragments $C_3H_2N_2^+$, $C_3H_3N_2^+$, and $C_3H_4N_2^+$, respectively. It should be particularly concerned that these peaks at *m/z* 30, 49, and 68 could also have contributions from BF^+, BF_2^+, and BF_3^+, respectively.

From Figs. 7 and 8, it can also be seen that LAB103 were more sensitive to the frictional stimulus than LB104. During the friction process, it seemed that various spectral components exhibited obviously different intensities. Once the friction process ended, hydrogen and most of these alkanes and alkenes radicals decreased precipitously. However,

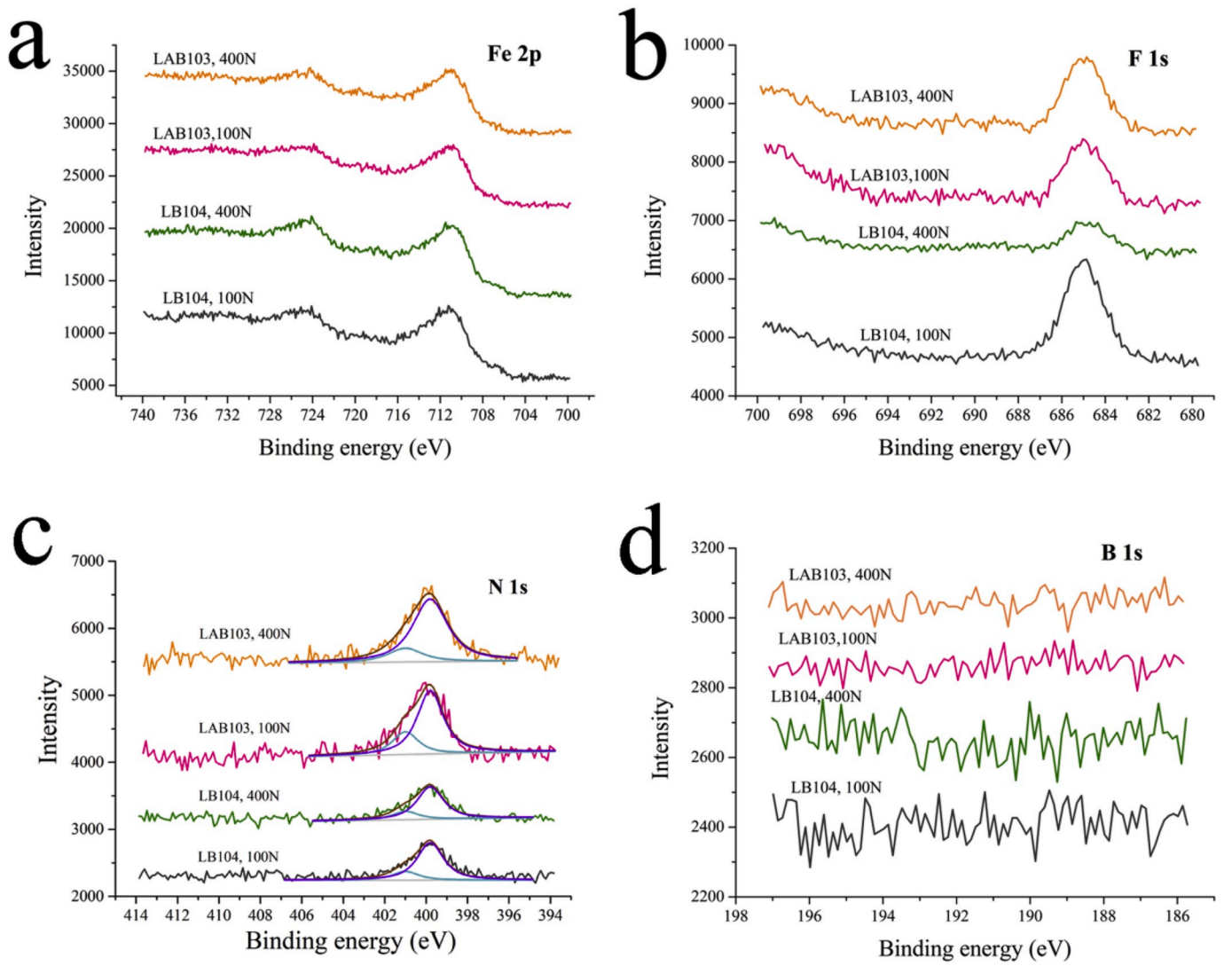

Fig. 5. XPS spectra of representative elements on the worn surface lubricated by LB104 and LAB103 under low and high loads: (a) Fe 2p; (b) F 1s; (c) N 1s; (d) B 1s.

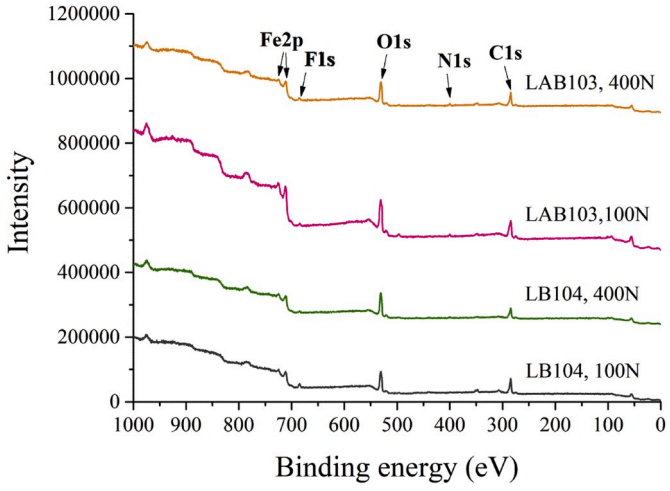

Fig. 6. XPS survey spectra of the worn surface lubricated by LB104 and LAB103 under low and high loads.

hetero atom-containing products, such as carbon-monoxide, carbon dioxide, imidazole and N-methylimidazole, could exist in the vacuum chamber for a long time.

In order to get deeper insights into these emission behaviors of ion fragments, the signal variations of DMS detections as functions of time were done. All these emission behavior types (BTs) of ion fragments were sorted as I, II, III, IV, V and VI, based on the following clarification rules: '*sharp increase at the start of the friction process*', '*dynamic equilibrium state during the friction process*', '*sudden decrease after the friction process*' and '*fall into initial state (zero) in minutes after the friction process*'. All the BT results of two ILs under different loads were listed in Table 2. To make it easier to understand, Fig. 9 presents some typical BTs of these ion fragments. As shown in Figs. 9a and 9b, BT I is used to describe the emission behavior like that the signals quickly achieved the dynamic equilibrium state after a sharp increase at the start of the friction process. The equilibrium state could be kept until a sudden decrease after the end of the friction process, and then fell into the initial value within tens of seconds. BT II in Figs. 9c and 9d was similar to BT I except that the signal intensity could not fall back into the initial state after the end of the friction process, even at 10 min later. BT III represented the emission behaviors of imidazole $C_3H_2N_2$+with *m/z* 66 of LAB103 under 400 N in Figs. 9e and 9f, which was also similar to pattern I. The only difference is that the emission intensity gradually increased during the whole frictional process without the dynamic equilibrium state. For the

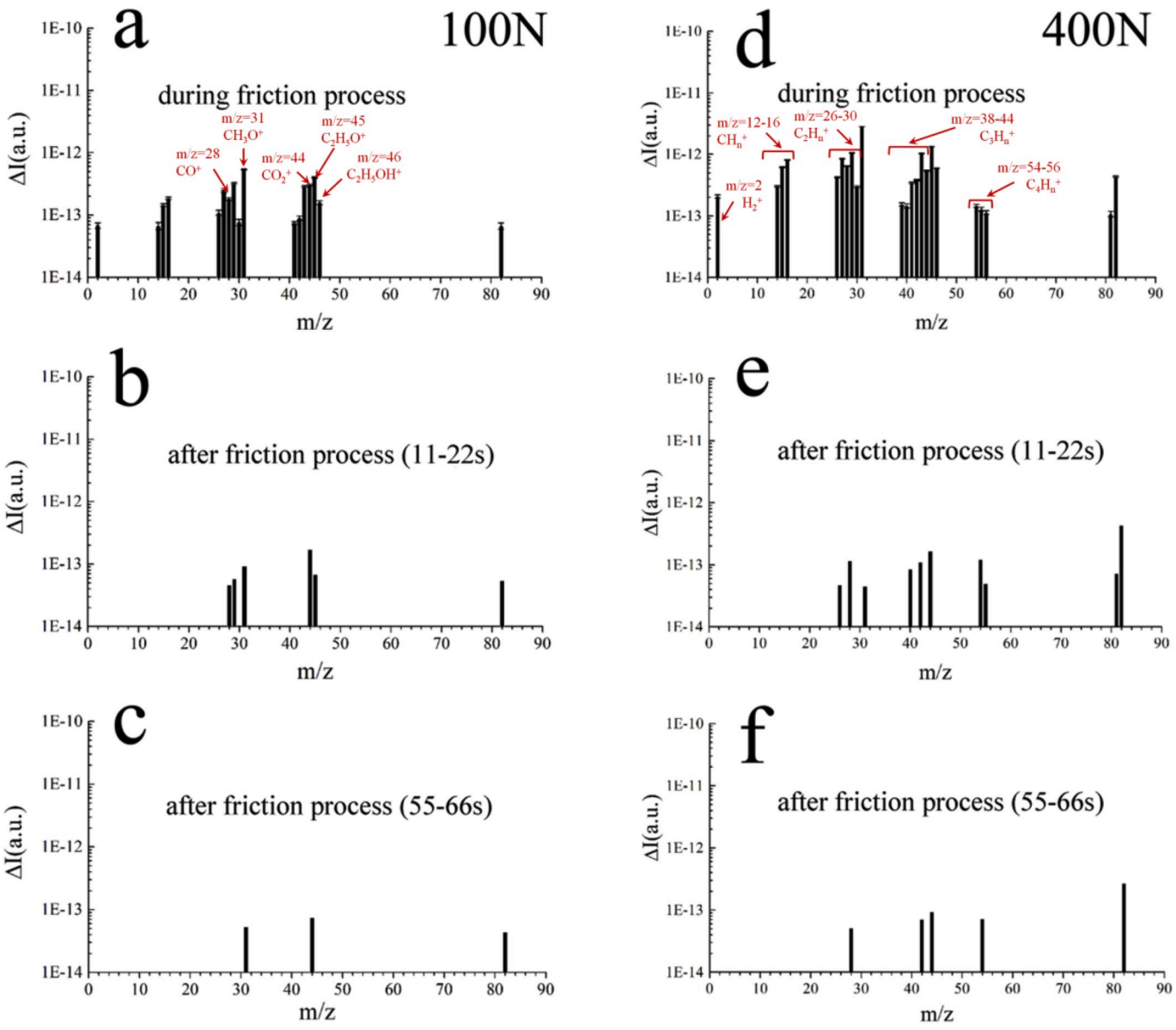

Fig. 7. DMS spectra for LB104 under the load of 100 N (a–c) and 400 N (d–f): during friction process (a, d); after the friction process ended (b, e) 11–22s, (c, f) 55–66s.

ion fragments in Figs. 9g and 9h, pattern IV is characterized by generating a new nonzero dynamic equilibrium state after the end of friction process, which is similar to BT III. For the ion fragments in Figs. 9i and 9j, BT V is similar to BT III other than the addition to a sharp increase at the start of friction process. The signals of N-methylimidazole [$(C_3H_3N_2)CH_3$] $^+$) at *m/z* 82 performed as BT VI. The increase at the start of the friction process was so gentle that a dynamic equilibrium state could not be obtained during the friction process. Additionally, the decrease after the end of the friction process was also slow and the signal could not fall back into initial state (zero) even after approximately 10 min.

These results of DMS spectra and clarification of BTs are definitely useful for analyzing the decomposition process of either cationic or anionic parts of IL molecules under different frictional stimulus. According to the QMS results, it could be deduced that the main products emitted during frictional stimulus process of LB104 would be CH_4, C_4H_{10}, CH_3F, and N-methylimidazole $(C_3H_3N_2)CH_3$. Besides these emission products, new products imidazole BF_3 and $C_3H_3N_2$ were detected for LAB103. In addition, these O-containing volatile components, CO_2, CH_3OH, and C_2H_5OH, were related with the recombination of some existing radicals. However, limited results can be concluded in present work, much more work need to be done in the future to obtain a deeper insight to the tribo-decomposition mechanisms.

4. Discussion

Many factors, which might affect the tribo-degradation process of ILs, have been discussed and verified by researchers [24,25]. The following two could be surely excluded: frictional heating and catalytic effect of fresh metal surfaces [26]. In the viewpoint of Nevshupa et al. [25,26], the bond dissociation and formation of ions and radicals can be occurred by mechanical stimulation on the tribo-contact zone, which could provide highly concentrated mechanical energy to the IL. Some of the ions and radicals arrived at QMS directly or recombination on the way to QMS, and others participated in the tribochemical reactions with the substrate surface, producing various tribo-products on the worn surfaces.

Considering these results and discussions, the possible mechanisms of tribo-degradation and tribochemical reactions of the ILs were

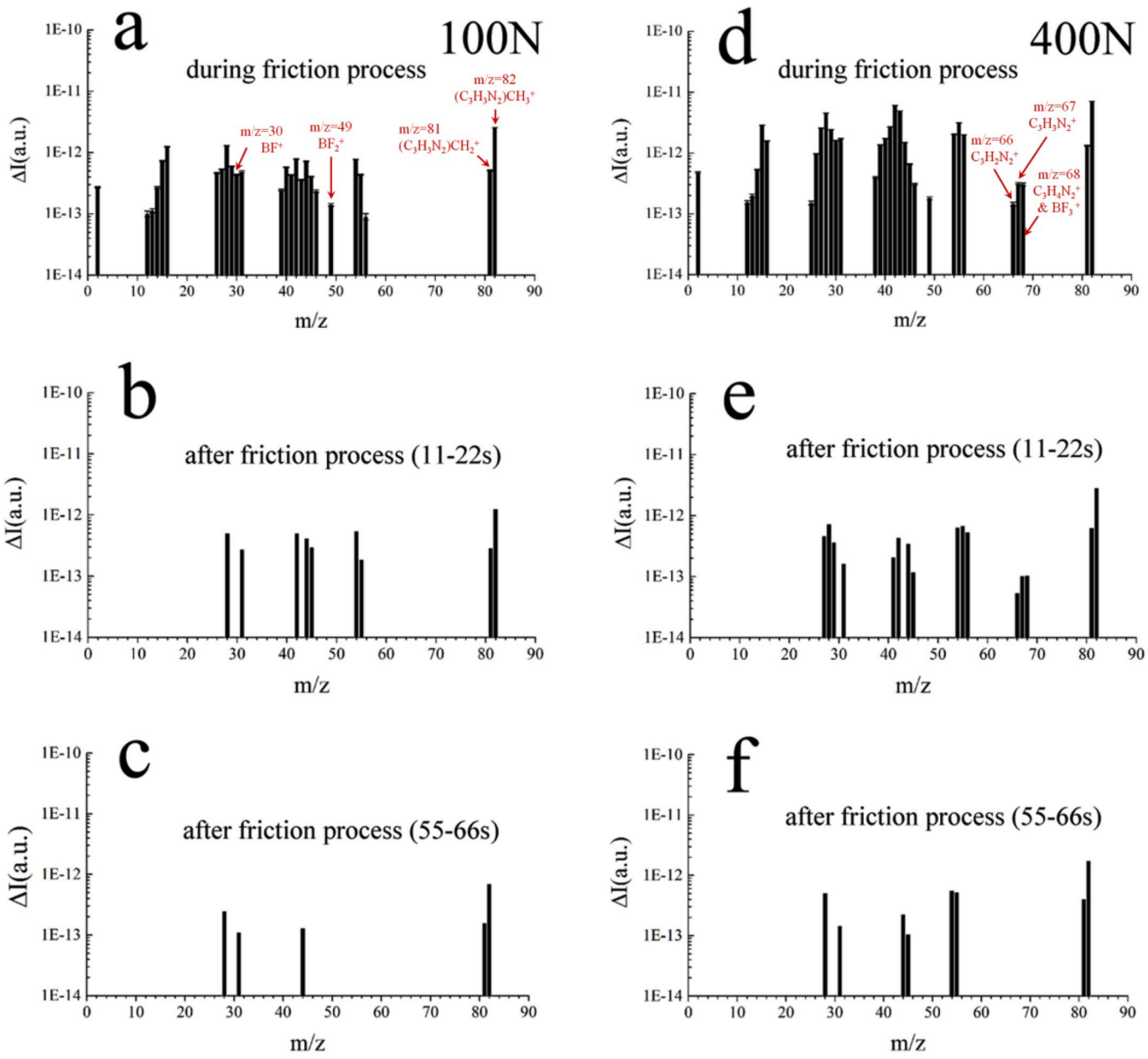

Fig. 8. DMS spectra for LAB103 under the load of 100 N (a–c) and 400 N (d–f): during friction process (a, d); after the friction process ended (b, e) 11–22s, (c, f) 55–66s.

proposed in Fig. 10. Generally, the rubbing of steel substrate surfaces under the tribo-stress can induce the positive charge [27]. BF_4^- anions, as the anionic moiety of both ILs, preferentially adsorbed on the surface of steel substrate by electrostatic attraction, which would lead to that the dissociation focuses on the fracture of B–F bond. For the cationic moieties of two ILs, the adsorption layers are formed through either the electrostatic attraction with BF_4^- or the combination of imidazole ring or vinyl on the steel surfaces. When cationic moieties adsorbed on the steel surfaces mainly through the imidazole ring, the regularity of ILs' adsorption layers will be disturbed due to the steric hindrance. In this case, it will make the attack of corrosive products to steel surface easier. In addition, the degradation of cationic moieties was concentrated on detachment of side alkyl, including butyl, allyl, and methyl, rather than on the ring-opening of imidazole. The tribo-degradation products partially diffused to the QMS, exciting various MS signals, and the others participated in the generation of tribofilms through tribochemical reactions on the worn surfaces.

For LB104, it could be found that no signals about BF_3 were detected by QMS detector, but intensive tribochemical reactions induced severe corrosion wear and excessive FeF_2 were formed on the worn surfaces. It demonstrates that the majority of tribo-degradation products of the anionic moiety participated in the tribochemical reactions, producing thick tribofilms of FeF_2 under 100 N. However, the thick tribofilms could not be kept during the friction process, due to the high contact stress and overconsumption of FeF_2 layer at 400 N. For the tribofilms originated from cationic moiety of LB104, thin films of N-containing compounds were generated inside the contact area both at lower and higher loads, but the tribo-films were not thick enough to prevent the worn surfaces from the attack of F^- and BF_3. For LAB103, on the account of the vinyl functionalized group, the attack of F^- and BF_3 to the steel surfaces could be effectively alleviated. Hence, the steel worn surfaces were mainly covered by N-containing compounds and a few tribochemical products FeF_2.

Table 2
Summary of various BTs of ion fragments of two ILs under different loads.

BTs	LB104		LAB103	
	100 N	400 N	100 N	400 N
I	2, 14, 16	2, 14, 16, 45, 46	2	2, 12–14, 16
II	15	15, 31		15
III	26, 27, 29, 30	26, 27, 29, 30, 56	12-14, 16, 43, 49, 56	25, 45, 46, 49, 66
IV	28, 31, 41-46	28, 39-44	15, 26–31, 44-46	26-31, 38–44, 54–56, 67–68, 81
V		82, 54	39-42, 54, 55, 81, 82	82
VI	82	55, 81		

Notes: these *m/z* values listed in this table could be ascribed to the following ion fragments, 2: H_2^+; 12–16: CH_x^+ (x = 0–4); 26–30: $C_2H_y^+$ (y = 2–6); 38–44: $C_3H_z^+$ (z = 2–8); 28, 44: CO^+, and CO_2^+; 31, 45, 46: CH_3O^+, $C_2H_5O^+$, and $C_2H_5OH^+$; 54–56: $C_4H_7^+$, $C_4H_8^+$, and $C_4H_9^+$; 66–68: $C_3H_2N_2^+$, $C_3H_3N_2^+$, and $C_3H_4N_2^+$; 81, 82: $[(C_3H_3N_2)CH_2]^+$, and $[(C_3H_3N_2)CH_3]^+$; 30, 49, 68: BF^+, BF_2^+, and BF_3^+.

5. Conclusion

In this work, two imidazolium tetrafluoroborate ILs with alkyl and alkenyl were comparatively studied on their vacuum lubrication properties, and tribo-decomposition behaviors. The conclusions can be drawn as follows:

(1) Both ILs present quite wide liquid ranges with high thermal stability, low pour point and extremely low glass transition temperatures.
(2) LB104 corrodes the steel surface seriously during the friction process, while vinyl functionalized ILs LAB103 can effectively prevent the worn surface from corrosive attack, yielding better lubrication properties, especially under higher load.
(3) The better lubrication performance of LAB103 should be ascribed to the combination of adsorption layers consisting of ILs and tribochemical films including N-containing compounds and FeF_2.
(4) The decomposition behaviors of cationic moieties for both ILs are mainly due to the detachment of side alkyl, including butyl, allyl,

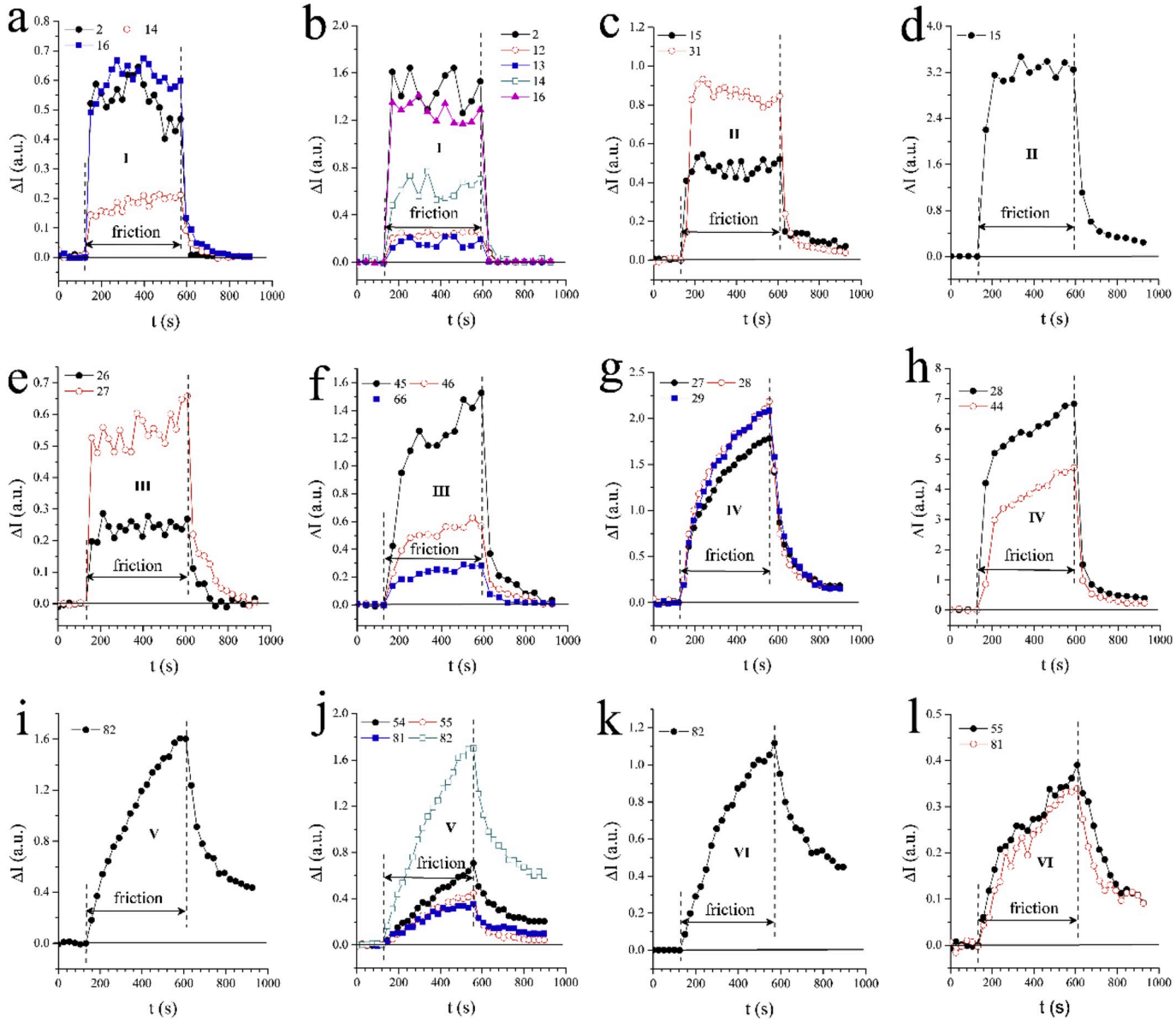

Fig. 9. Some of the most representative BTs of the ion fragments of two ILs as a function of time: (a, k) LB104, 100 N; (c, e, i, l) LB104, 400 N; (g, j) LAB103, 100 N; (b, d, f, h) LAB103, 400 N.

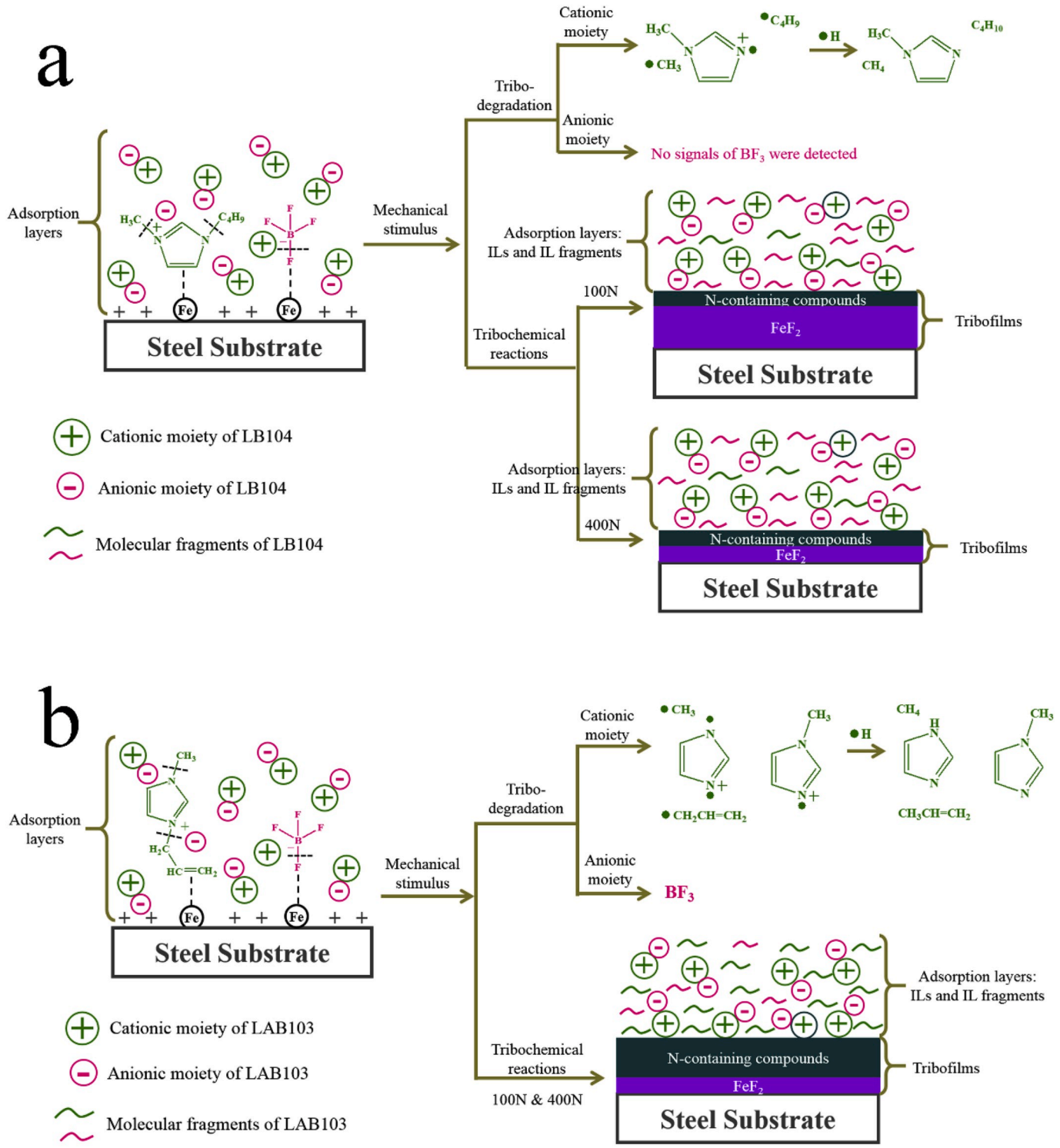

Fig. 10. The possible mechanisms of tribo-degradation and tribochemical reactions of two ILs: (a) LB104; (b) LAB103.

and methyl, rather than on the ring-opening of imidazole. For anionic moieties of both ILs, the decomposition behaviors are focused on the fracture of B–F bond, but these volatile components of two ILs are obviously different.

(5) The majority of anionic decomposition products of LB104 participated in the tribochemical reactions with steel substrate surfaces. For LAB103, limited F^- participated in the tribochemical reactions, while others formed the volatile components BF_3.

Declaration of competing interest

The authors declare that they have no known competing financial interests or personal relationships that could have appeared to influence the work reported in this paper.

CRediT authorship contribution statement

Yi Li: Methodology, Investigation, Data curation, Writing - original

draft. **Songwei Zhang:** Conceptualization, Funding acquisition, Writing - review & editing, Supervision. **Qi Ding:** Investigation, Formal analysis, Funding acquisition. **Litian Hu:** Resources, Funding acquisition, Project administration, Supervision.

Acknowledgements

This work was supported by the National Natural Science Foundation of China (51575506 and 51705508) and Beijing Key laboratory of Long-life Technology of Precise Rotation and Transmission Mechanisms (BZ0388201802).

References

[1] Jones Jr WR, Jansen MJ. Lubrication for space applications. 2005. NASA/CR-213424.
[2] Wang H, Zhang S, Qiao D, Feng D, Liu W. Tribological performance of silahydrocarbons used as steel-steel lubricants under vacuum and atmospheric pressure. J Nanomater 2014;852386:8.
[3] Ye C, Liu W, Chen Y, Yu L. Room-temperature ionic liquids: a novel versatile lubricant. Chem Commun 2001:2244–5.
[4] Zhou F, Liang Y, Liu W. Ionic liquid lubricants: designed chemistry for engineering applications. Chem Soc Rev 2009;38:2590–9.
[5] Yu B, Bansal DG, Qu J, Sun X, Luo H, Dai S, et al. Oil-miscible and non-corrosive phosphonium-based ionic liquids as candidate lubricant additives. Wear 2012;289:58–64.
[6] Somers AE, Howlett PC, MacFarlane DR, Forsyth M. A review of ionic liquid lubricants. Lubricants 2013;1:3–21.
[7] Li Y, Zhang S, Ding Q, Feng D, Qin B, Hu L. The corrosion and lubrication properties of 2-Mercaptobenzothiazole functionalized ionic liquids for bronze. Tribol Int 2017;114:121–31.
[8] Zhou Y, Qu J. Ionic liquids as lubricant additives: a review. ACS Appl Mater Interfaces 2017;9:3209–22.
[9] Masuko M, Mizuno H, Suzuki A, Obara S, Sasaki A. Lubrication performance of multialkylatedcyclopentane oils for sliding friction of steel under vacuum condition. J Synth Lubric 2007;24:217–26.
[10] Zhang S, Hu L, Wang H, Feng D. Tribological behaviors of several synthetic hydrocarbons in vacuum. Tribology 2011;31:569–74.
[11] Zhang S, Hu L, Wang H, Feng D. Tribological behaviors of two kinds of fluorine-containing space lubricating oil in vacuum. Tribology 2012;32:619–25.
[12] Zhang S, Hu L, Qiao D, Feng D, Wang H. Vacuum tribological performance of phosphonium-based ionic liquids as lubricants and lubricant additives of multialkylated cyclopentanes. Tribol Int 2013;66:289–95.
[13] Han Y, Qiao D, Zhang S, Feng D. Influence of phosphate and phosphonate ionic liquid structures on lubrication for different alloys (Mg, Al, Cu). Tribol Int 2017;114:469–77.
[14] Li Y, Zhang S, Ding Q, Li H, Qin B, Hu L. Understanding the synergistic lubrication effect of 2-mercaptobenzothiazolate based ionic liquids and Mo nanoparticles as hybrid additives. Tribol Int 2018;125:39–45.
[15] Matczak L, Johanning C, Gil E, Guo H, Smith TW, Schertzer M, et al. Effect of cation nature on the lubricating and physicochemical properties of three ionic liquids. Tribol Int 2018;124:23–33.
[16] Amiril SAS, Rahim EA, Embong Z, Syahrullail S. Tribological investigations on the application of oil-miscible ionic liquids additives in modified Jatropha-based metalworking fluid. Tribol Int 2018;120:520–34.
[17] Nevshupa R, Conte M, del Campo A, Roman E. Analysis of tribochemical decomposition of two imidazolium ionic liquids on Ti–6Al–4V through Mechanically Stimulated Gas Emission Spectrometry. Tribol Int 2016;102:19–27.
[18] Nevshupa R, Conte M, Guerra S, Roman E. Time-resolved characterization of dynamic tribochemical processes for dicationic imidazolium ionic liquid. Lubricants 2017;5:27.
[19] Kawada S, Watanabe S, Tadokoro C, Tsuboi R, Sasaki S. Lubricating mechanism of cyano-based ionic liquids on nascent steel surface. Tribol Int 2018;119:474–80.
[20] Bonhôte P, Dias A-P, Papageorgiou N, Kalyanasundaram K, Grätzel M. Hydrophobic, highly conductive ambient-temperature molten salts. Inorg Chem 1996;35:1168–78.
[21] Naumkin AV, Vass AK, Gaarenstroom SW, Powell CJ. NIST X-ray photoelectron spectroscopy database,NIST Standard Reference Database 20. 2012. Version 4.1.
[22] Lu R, Mori S, Kobayashi K, Nanao H. Study of tribochemical decomposition of ionic liquids on a nascent steel surface. Appl Surf Sci 2009;255:8965–71.
[23] Nevshupa RA, Roman E, de Segovia JL. Contamination of vacuum environment due to gas emission stimulated by friction. Tribol Int 2013;59:23–9.
[24] Jiménez AE, Bermúdez MD. Ionic liquids as lubricants of titanium–steel contact. Tribol Lett 2009;33:111–26.
[25] Nevshupa RA. The role of athermal mechanisms in the activation of tribodesorption and triboluminisence in miniature and lightly loaded friction units. J Frict Wear 2009;30:118–26.
[26] Mahrova M, Conte M, Roman E, Nevshupa R. Critical insight into mechanochemical and thermal degradation of imidazolium-based ionic liquids with alkyl and monomethoxypoly(ethylene glycol) side chains. J Phys Chem C 2014;118:22544–52.
[27] Kajdas C. Importance of anionic reactive intermediates for lubricant component reactions with friction surfaces. Lubric Sci 1994;6:203–28.